Fitoterapia 162 (2022) 105297

Contents lists available at ScienceDirect

Fitoterapia

journal homepage: www.elsevier.com/locate/fitote

Antimicrobial secondary metabolites from an endophytic fungus *Aspergillus polyporicola*

Si-Si Liu [a], Rong Huang [b], Shou-Peng Zhang [a], Tang-Chang Xu [a], Kun Hu [c], Shao-Hua Wu [a,*]

[a] State Key Laboratory for Conservation and Utilization of Bio-Resources in Yunnan, and Key Laboratory for Microbial Resources of the Ministry of Education, Yunnan Institute of Microbiology, School of Life Sciences, Yunnan University, Kunming 650091, China
[b] School of Chemical Science and Technology, Yunnan University, Kunming 650091, China
[c] State Key Laboratory of Phytochemistry and Plant Resources in West China, Kunming Institute of Botany, Chinese Academy of Sciences, and Yunnan Key Laboratory of Natural Medicinal Chemistry, Kunming 650201, China

ARTICLE INFO

Keywords:
Endophyte
Aspergillus polyporicola
Nucleoside
Cyclohexanone
Antimicrobial activity

ABSTRACT

Two new nucleoside derivatives, kipukasins O (**1**) and P (**2**), one new cyclohexenone derivative, arthropsadiol D (**5**), and one new natural product, (+)-2,5-dimethyl-3(2H)-benzofuranone (**6**), together with eleven known compounds (**3**, **4**, **7**–**15**), were obtained from the culture broth of the endophytic fungus *Aspergillus polyporicola* R2 isolated from the roots of *Synsepalum dulcificum*. Among them, the absolute configuration of compound **5** was determined by quantum chemical calculations of NMR chemical shifts and ECD spectrum. The antimicrobial activities of these compounds were evaluated. Compound **11** exhibited obvious inhibitory activity against MRSA, *Staphylococcus aureus*, *Salmonella typhimurium*, *Botrytis cinerea*, and *Fusarium graminearum* with MIC values of 4, 4, 4, 32, and 16 μg/mL, respectively. Compound **12** exhibited antibacterial activity against *S. typhimurium* and MRSA with MIC values of 4 and 16 μg/mL. Compound **6** exhibited antifungal activity against *F. graminearum* with MIC value of 32 μg/mL.

1. Introduction

Endophytic fungi live in the healthy tissues of plants and do not cause significant symptoms in the host plants [1]. They can produce abundant secondary metabolites with a variety of structural types and biological activities [2]. They are ubiquitous in nature and highly effected by climatic conditions and the host plant's location [3]. Endophytic fungi associated with medicinal plants are a potential source for discovering new biological substances, which can be used as pharmaceutical and agrochemical drugs [4].

The tropical plant *Synsepalum dulcificum* is attractive for its pulp which can transform sourness into sweetness and called as "miracle fruit" [5]. Pharmacological studies have shown that the extracts of *S. dulcificum* possessed the effects of antioxidant [6], blood sugar regulation [7] and blood lipid lowering [8]. Some studies have proved that the antimicrobial effect of *S. dulcificum* extracts on *Staphylococcus aureus*, *Bacillus subtilis*, *Proteus vulgaris* and *Listeria monocytogenes*, etc. [9,10]. In addition, this plant is often used to treat diabetes and diarrhea in folk medicine. The chemical components of *S. dulcificum* mainly included miraculin [11], fatty acids and their esters [12], polyphenols [13], terpenes [14], and sterols [15].

Till now, there is no report on endophytes from *S. dulcificum*. Our recent research work is focused on isolating endophytic fungi from *S. dulcificum* and antimicrobial screening of these fungal strains. As one of the results, the culture extract of the strain *Aspergillus polyporicola* R2 showed obvious antimicrobial activity against *Salmonella typhimurium*, *S. aureus*, and *Fusarium moniliforme*. Fungi in the genus *Aspergillus* could produce a variety of bioactive secondary metabolites, such as antiviral asperterrestide A [16], antimalarial butyrolactone V [17], cytotoxic rubasperone D [18], and versicolor A [19], as well as the important antibiotics penicillins [20]. *Aspergillus* species has become a research hotspot in recent years due to its potent ability of synthesizing rich bioactive molecules. Among them, *A. polyporicola*, as an uncommon species, has only been reported to produce cytochalasin and curvularin derivatives at present [21,22].

In this study, the chemical investigation on fermentation broth of the strain R2 resulted in two new nucleoside derivatives, kipukasins O (**1**) and P (**2**), one new cyclohexenone derivative, arthropsadiol D (**5**), and one new natural product, 2,5-dimethyl-3(2H)-benzofuranone (**6**), together with eleven known compounds, including kipukasin C (**3**) [23],

* Corresponding author.
E-mail address: shwu123@126.com (S.-H. Wu).

https://doi.org/10.1016/j.fitote.2022.105297
Received 8 July 2022; Received in revised form 2 September 2022; Accepted 3 September 2022
Available online 9 September 2022

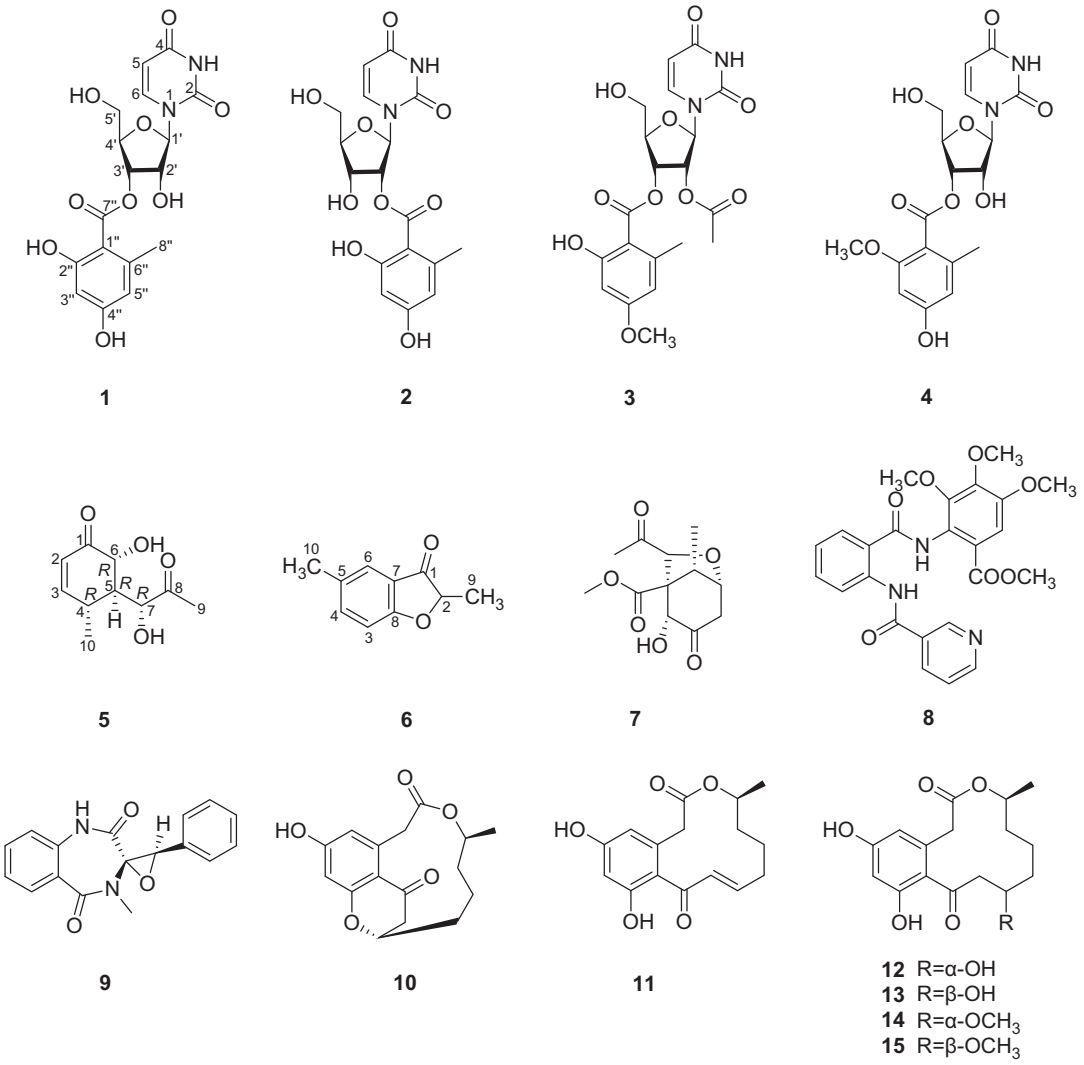

Fig. 1. Chemical structures of compounds **1**–**15.**

kipukasin I (**4**) [24], massarilactone G (**7**) [25], methyl 3,4,5-trimethoxy-2-(2-(nicotinamido)benzamido) benzoate (**8**) [26], cyclopenin (**9**) [27], curvulopyran (**10**) [21], 11-dehydrocurvularin (**11**) [28], 11α-hydroxycurvularin (**12**) [29], 11β-hydroxycurvularin (**13**) [29], 11α-methoxycurvularin (**14**) [30], and 11β-methoxycurvulain (**15**) [30] (Fig. 1). The absolute configuration of compound **5** was determined by quantum chemical calculations of NMR chemical shifts and ECD spectrum. Furthermore, the antimicrobial activities of these compounds were also described in this paper.

2. Experimental

2.1. General experimental procedures

The optical rotation was measured using a Jasco P-2000 polarimeter. The infrared (IR) spectra were recorded on a Bio-Rad FTS spectrometer using KBr pellets. UV spectra were recorded on Shimadzu double-beam 210A spectrophotometer. NMR spectra were acquired using a Bruker DRX-600 spectrometer, using TMS as internal standard. HRESIMS spectra were obtained from an Agilent G3250AA LC-MSD TOF mass spectrometer. ECD data were acquired from an Agilent Applied Photophysics circular dichroism spectrometer. Column chromatography (CC) was carried out on Sephadex LH-20 (Pharmacia), silica gel type 200–300 mesh (Qingdao Marine Chemical Inc., China), and RP-18 silica gel (40–63 μm, Merck).

2.2. Microbial material

The strain R2 was isolated from the roots of *S. dulcificum* collected in October 2018 from Xishuangbanna Botanical Garden in Yunnan Province, China. The strain was identified as *A. polyporicola* based on the analysis of its partial ITS gene sequence (accession No. ON557670) and deposited in Yunnan Institute of Microbiology, Yunnan University, P. R. China.

2.3. Fermentation and extraction

The activated strain was transferred into 500 mL Erlenmeyer flasks which contained 100 mL of PDB liquid medium (×50) at 28 °C for 3 days, with a rotation speed of 200 rpm. Each of the seed cultures (25 mL) was transferred into 1000 mL Erlenmeyer flasks (×200) containing 250 mL of PDB medium and cultured at 28 °C for 11 days on a rotary shaker at 200 rpm. The filtered fermentation broth (50 L) was concentrated under reduced pressure to a volume of 10 L and then exhaustively extracted with an equal volume of EtOAc for four times. The combined organic phase was then concentrated in vacuo to obtain a brown gum of crude extract (13 g).

Table 1
^{1}H and ^{13}C NMR data of compounds **1** and **2** in pyridine-d_5.

Position	**1**		**2**	
	δ_H (J in Hz)	δ_C	δ_H (J in Hz)	δ_C
2		152.0, C		152.0, C
4		163.9, C		163.9, C
5	5.78 (d, 8.1)	102.8, CH	5.85 (d, 8.1)	102.9, CH
6	8.42 (d, 8.1)	140.4, CH	8.51 (d, 8.1)	140.6, CH
1′	6.88 (d, 6.1)	89.5, CH	7.04 (d, 5.2)	87.3, CH
2′	5.29 (t, 5.8)	73.4, CH	6.19 (t, 5.3)	77.7, CH
3′	6.12 (dd, 5.3, 3.4)	74.8, CH	5.29 (t, 5.8)	69.6, CH
4′	4.73 (q, 2.4)	83.8, CH	4.64 (q, 2.1)	87.0, CH
5′	a: 4.27 (dd,12.1, 2.2) b: 4.21 (dd,12.1, 2.4)	61.6, CH_2	a: 4.31 (dd, 12.1, 2.3) b: 4.17 (dd, 12.1, 2.4)	61.6, CH_2
1″		105.6, C		105.6, C
2″		164.1, C		164.1, C
3″	6.78 (d, 2.3)	101.8, CH	6.71 (d, 2.4)	101.6, CH
4″		165.1, C		165.1, C
5″	6.63 (d, 1.8)	112.5, CH	6.58 (d, 1.8)	112.5, CH
6″		143.9, C		144.1, C
7″		170.6, C		170.6, C
8″	2.78 (s)	24.0, CH_3	2.81 (s)	24.1, CH_3

Table 2
^{1}H and ^{13}C NMR data of compounds **5** and **6.**

Position	**5**[a]		**6**[b]	
	δ_H (J in Hz)	δ_C	δ_H (J in Hz)	δ_C
1		199.6, C		206.3, C
2	6.08 (dd, 10.1, 2.9)	124.5, CH	4.93 (q, 7.0)	70.7, CH
3	6.75 (dd, 10.1, 2.0)	157.4, CH	7.08 (d, 8.5)	132.4, CH
4	3.03 (m)	31.4, CH	6.83 (dd, 8.5, 2.5)	118.1, CH
5	2.26 (d, 12.4)	53.0, CH		127.9, C
6	4.30 (d, 12.4)	72.6, CH	6.97 (d, 2.5)	114.3, CH
7	4.66 (s)	75.5, CH		136.7, C
8		211.4, C		155.0, C
9	2.32 (s)	25.8, CH_3	1.27 (d, 7.0)	19.0, CH_3
10	1.02 (d, 7.3)	19.0, CH_3	2.28 (s)	18.3, CH_3

[a] Measured in $CDCl_3$.
[b] Measured in CD_3OD.

2.4. Isolation and purification

The extract was submitted to silica gel CC, eluting with a gradient of $CHCl_3$/MeOH from 1:0 to 0:1 (v/v) to obtain four fractions (Frs. 1–4). Fr.1 was subjected to silica gel CC (petroleum ether/EtOAc) from 9:1 to 1:1 to obtain Fr. 1.1 and Fr. 1.2. Fr. 1.1 was further purified by silica gel CC ($CHCl_3$/MeOH 75:1) to afford compound **8** (3 mg). Fr. 1.2 was separated by silica gel CC ($CHCl_3$/MeOH 50:1) and further purified by RP-18 CC (MeOH/H_2O 4:6) to afford **6** (7 mg) and **9** (3 mg). Fr. 2 was further purified by silica gel CC (petroleum ether/acetone 8:2) to afford Frs. 2.1–2.2. Fr. 2.1 was repeatedly subjected to silica gel CC ($CHCl_3$/MeOH 30:1) to afford compound **7** (2 mg). Fr. 2.2 was purified by RP-18 CC (MeOH/H_2O 3:7) to afford compound **10** (2 mg). Fr. 3 was repeatedly subjected to silica gel CC ($CHCl_3$/MeOH 20:1) to afford Frs. 3.1–3.3. Fr. 3.1 was further purified by silica gel CC (petroleum ether/acetone 7:3) to afford compounds **11** (10 mg) and **14** (3 mg). Fr. 3.2 was subjected to silica gel CC with petroleum ether/acetone (6:4) to afford compound **15** (2 mg). Compound **5** (3 mg) was yielded by silica gel CC ($CHCl_3$/MeOH 10:1) from Fr. 3.3. Fr. 4 was further purified by silica gel CC ($CHCl_3$/MeOH 9:1) to afford Frs. 4.1–4.4. Fr. 4.1 was purified by RP-18 CC (MeOH/H_2O 2:8) to afford compounds **3** (2 mg) and **4** (8 mg). Fr. 4.2 was chromatographed on silica gel column with $CHCl_3$/MeOH (8:2) and RP-18 silica gel with MeOH/H_2O (1:9) to afford compounds **1** (3 mg) and **2** (3 mg). Fr. 4.3 was further purified by silica gel CC (petroleum ether/acetone 1:1) to afford compound **12** (8 mg). Compound **13** (3 mg) was yielded by silica gel CC $CHCl_3$/MeOH (6:4) from Fr. 4.4.

2.4.1. Kipukasins O and P (1/2)

White solid; UV (MeOH) λ_{max} (log ε): 209 (3.16), 258 (1.78) nm; IR (KBr) ν_{max} 3450, 3260, 2934, 1716, 1682, 1618, 1579, 1468, 1447, 1410, 1382, 1327, 1256, 1175, 1139, 1098, 1068, 991, 916 cm^{-1}; ^{1}H and ^{13}C NMR spectral data, see Table 1; HRESIMS m/z 417.0903 $[M + Na]^+$ (calcd for $C_{17}H_{18}N_2NaO_9$, 417.0910).

2.4.2. Arthropsadiol D (5)

Colorless crystal; [α]20 D = −106.0 (c 0.15, MeOH); UV (MeOH) λ_{max} (log ε): 235 (3.29) nm; IR ν_{max} 3425, 2962, 2925, 1713, 1694, 1382, 1239, 1099, 1065, 909 cm^{-1}; ^{1}H and ^{13}C NMR spectral data, see Table 2; HRESIMS: m/z $[M + Na]^+$ 221.0784 (calcd for $C_{10}H_{14}NaO_4$, 221.0790).

2.4.3. 2,5-Dimethyl-3(2H)-benzofuranone (6)

Colorless oil; [α]20 D = −232.5 (c 0.55, MeOH); ^{1}H and ^{13}C NMR spectral data, see Table 2; HRESIMS: m/z $[M + H]^+$ 163.0761 (calcd for $C_{10}H_{11}O_2$, 163.0759).

2.5. Antimicrobial activity assay

The minimal inhibitory concentrations (MICs) of the isolated compounds were determined by the broth microdilution method [31]. Five pathogens were used, including methicillin-resistant *Staphylococcus aureus* (MRSA, YM 3106), *Staphylococcus aureus* (YM 3105), *Salmonella typhimurium* (YM 3115), *Botrytis cinerea* (YM 3061), and *Fusarium graminearum* (YM 3157). The pathogen suspension was loaded into each well of 96-well plates and various concentrations of compounds were added to give the final concentrations ranging from 512 to 1 μg/mL. Nystatin and chloramphenicol were used as positive control for fungus and bacteria, respectively.

3. Results and discussion

Compounds **1** and **2** were obtained as white solid. When detecting their NMR spectra, we observed an interesting transesterification reaction in which **1** and **2** rearranged rapidly to form each other, providing a **1**/**2** mixture in a ratio of about 2:1 in pyridine at room temperature.

The molecular formulas of both compounds **1** and **2** were determined as $C_{17}H_{18}N_2O_9$ from a quasi-molecular ion peak at m/z 417.0903 $[M + Na]^+$ (calcd for $C_{17}H_{18}N_2NaO_9$, 417.0910) in the HRESIMS, indicating the existence of ten degrees of unsaturation. The IR spectrum of **1** showed absorption bands for hydroxyl group (3450 cm^{-1}), amino group (3260 cm^{-1}), and three carbonyl groups (1716, 1682 and 1618 cm^{-1}). The ^{1}H and ^{13}C NMR spectra in pyridine-d_5 showed two sets of signals of compounds **1** and **2** with their approximate ratio of 2:1 (Table 1).

The ^{1}H NMR spectrum of the main component (**1**) revealed the presence of a 1,2,3,5-tetrasubstituted benzene ring (δ_H 6.78, d; δ_H 6.63, d), a 1,2-disubstituted olefin (δ_H 8.42, d; δ_H 5.78, d), four oxymethine protons (δ_H 4.73, 5.29, 6.12, 6.88), an oxymethylene group (δ_H 4.27, dd; δ_H 4.21, dd) and a methyl group (δ_H 2.78, s). The ^{13}C NMR spectrum revealed 17 carbon signals, including three carbonyl carbons (δ_C 152.0, 163.9, 170.6), four quaternary carbons (δ_C 105.6, 143.9, 164.1, 165.1), four olefinic methines (δ_C 101.8, 102.8, 112.5, 140.4), four oxymethines (73.4, 74.8, 83.8, 89.5,), one oxymethylene (δ_C 61.6) and a methyl group (δ_C 24.0). Besides the signals for a 1,2,3,5-tetrasubstituted benzene ring, the remaining ^{1}H and ^{13}C NMR signals could be attributed to a nucleoside moiety. The HMBC cross-peaks from H-6 (δ_H 8.42) to C-2 (δ_C 152.0), C-4 (δ_C 163.9), and C-5 (δ_C 102.8), and from H-5 (δ_H 5.78) to C-4 and C-6 (δ_C 140.4) suggested the presence of uracil unit (Fig. 2). A furanose moiety could be determined by the tracking correlations of four oxymethine protons and two splitted oxymethylene protons in the

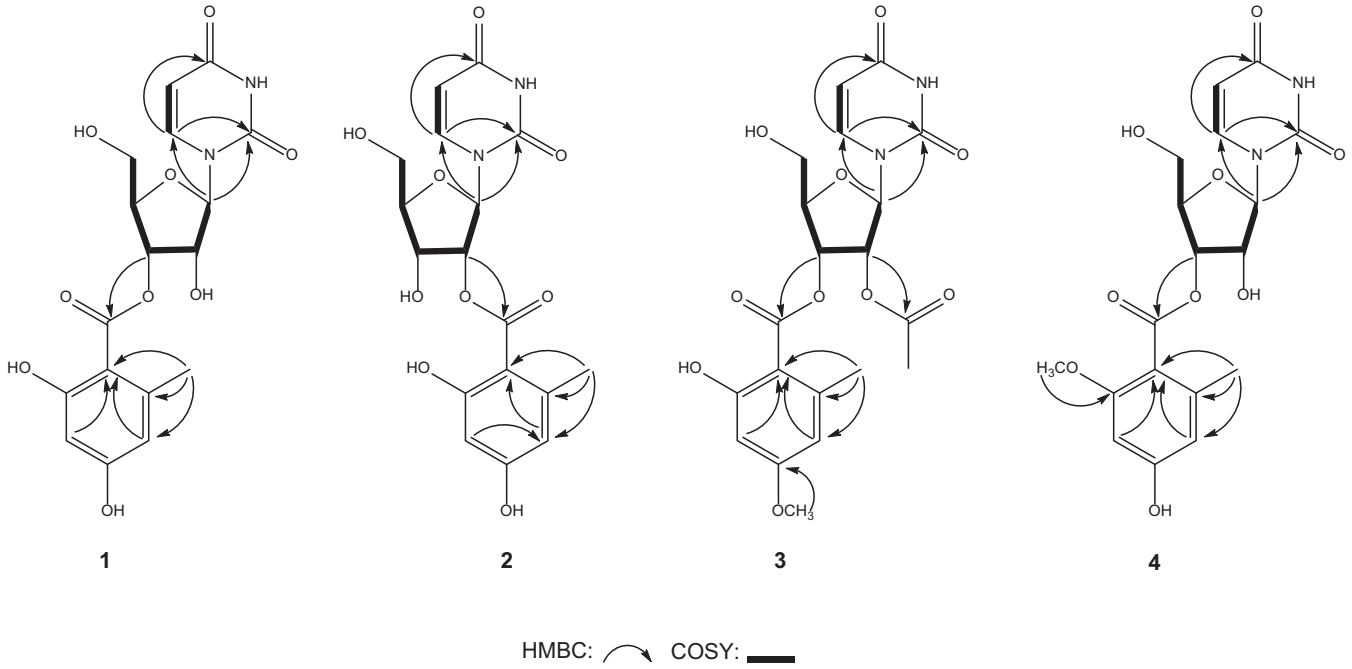

Fig. 2. Selected 2D NMR correlations of **1**–**4.**

^{1}H—^{1}H COSY spectrum (Fig. 2). The δ-value of the ^{1}H and ^{13}C NMR data (δ_H 6.88, d, J = 6.1 Hz; δ_C 89.5) indicated the existence of a C—N glycosidic linkage. The HMBC correlations from H-1′ to C-2 and C-6 further confirmed the connection of the furanose unit to the uracil moiety at the expected N-1 position. Thus, compound **1** had the skeleton of uracil-1-β-D-ribofuranoside, which was the same as kipukasin I [24], simultaneously reported as compound **4** in this paper. The main difference between **1** and **4** is the lack of a methoxy group in the aromatic

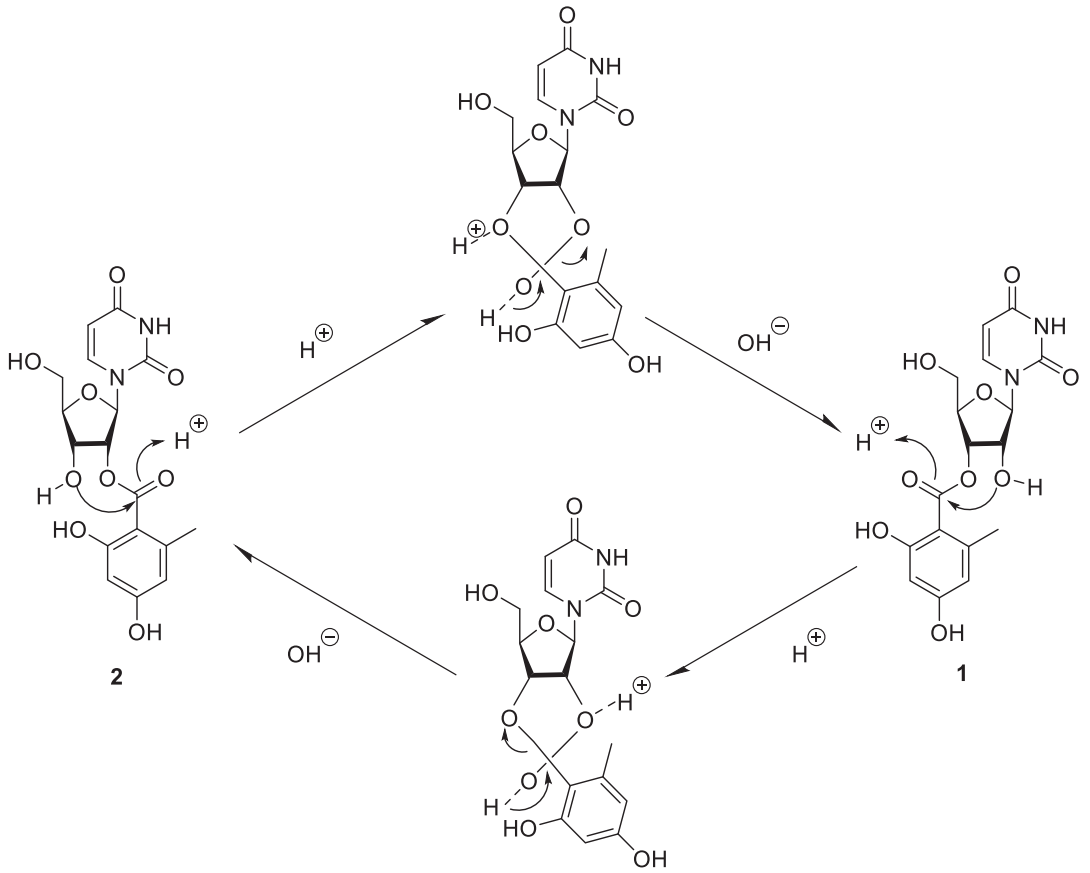

Fig. 3. Mechanism of the interconversion for **1** and **2** in pyridine.

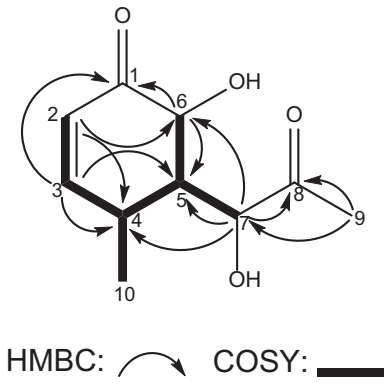

Fig. 4. Selected 2D NMR correlations of **5**.

ring, instead of a hydroxyl group in **1**, as supported by 14 amu less than that of **4**. The positions of the substitution in aromatic ring were determined by the analysis of NMR data and HMBC spectrum. The chemical shifts of C-3″ (δ_H 6.78; δ_C 101.8) were suggestive of oxygen substitution at both ortho positions. The methyl protons at δ_H 2.78 (s) showed HMBC correlations with C-1″, C-5″, and C-6″, indicating the location of the methyl group at C-6″. The carboxyl carbon C-7″ (δ_C 170.6) was connected to the sugar moiety through oxygen atom to form ester linkage. Although no correlations were observed for C-7″ to any protons in the HMBC spectrum, the position of the ester group could be determined by the chemical shift values. The signal for H-3′ was downfield shifted to δ_H 6.12 (dd, $J = 5.3$, 3.4 Hz) and H-2′ resonance was upfield shifted to δ_H 5.29 (t, $J = 5.8$ Hz), suggesting that the ester group was connected at C-3′, through the comparison of the spectral data between the tautomeric kipukasins H and I in the literature [24]. Based on the above analysis, the structure of **1** was determined as shown in Fig. 1 and named as kipukasin O.

The minor NMR spectral signals in the mixture of **1** and **2** were attributed to compound **2**. The ^{1}H and ^{13}C NMR spectra of **2** were very similar to those of **1**, differing only in the chemical shifts and splitting patterns of some of the ribose oxymethine proton signals in the ^{1}H NMR spectrum. The difference mainly showed that the downfield shift to δ_H 6.19 (t, $J = 5.3$ Hz) for H-2′ and upfield shift to δ_H 5.29 (t, $J = 5.8$ Hz) for H-3′ in **2**, indicating that the aroyl group was located at C-2′. Therefore, **2** is the regioisomer of **1**.

The absolute configurations of **1** and **2** were conjectured based on the biogenetic considerations. As mentioned above, the absolute configurations of the uridine moiety of compounds **1** and **2** could be assigned as uracil-1-β-D-ribofuranoside, which identical to the known nucleoside derivatives **3** and **4** [23].

This 2′/3′-transesterification has been reported to occur in some ribose derivatives [24]. In the process of the extraction and purification, the phenomenon of mutual conversion between **1** and **2** might be existed (Fig. 3). The 2'-*O*-acyl ribofuranoside or 3'-*O*-acyl ribofuranoside was unstable in pyridine when testing their NMR data and produced isomers by the interconversion via an acyl rearrangement. Regioisomer **2** was obtained by transferring the aroyl group from 3'-OH position in the ribose moiety of **1** to the adjacent 2'-OH via the semi-orthoester intermediate [32]. This aroyl migration was reversible and maintained a dynamic equilibrium.

Compound **5** was obtained as colorless crystal. It has the molecular formula $C_{10}H_{14}O_4$ as determined by HRESIMS at *m/z* 221.0784 $[M + Na]^+$ (calcd for $C_{10}H_{14}NaO_4$, 221.0790), indicating the existence of four degrees of unsaturation. Its IR spectrum showed absorption bands for a hydroxyl group (3425 cm^{-1}) and two carbonyl groups (1713, 1694 cm^{-1}). The ^{1}H, ^{13}C and HSQC NMR spectra (Table 2) exhibited a doublet methyl group (δ_H 1.02, d, $J = 7.3$ Hz; δ_C 19.0), a singlet methyl group (δ_H 2.32, s; δ_C 25.8), two carbonyls (δ_C 199.6, 211.4), a 1,2-disubstituted olefin (δ_H 6.08, dd, $J = 10.1$, 2.9 Hz, δ_C 124.5; δ_H 6.75, dd, $J = 10.1$, 2.0 Hz, δ_C 157.4) and two oxymethine groups (δ_H 4.30, d, $J = 12.4$ Hz, δ_C 72.6; δ_H 4.66, s, δ_C 75.5). Since two carbonyl groups and a double bond accounted for three degrees of unsaturation, the remaining one revealed the presence of a single ring in **5**.

Table 3
The results for NMR computation of **5a*** and **5b***.

Atom type	Parameter	5a*	5b*
	R^{2a}	0.9994	0.9991
^{13}C	MAE [b] (ppm)	1.7	2.5
	CMAE [c] (ppm)	1.4	1.8
	R^2	0.9968	0.9843
^{1}H	MAE (ppm)	0.18	0.18
	CMAE (ppm)	0.09	0.16

[a] R^2: Squared Pearson correlation coefficient between experimental and calculated NMR chemical shifts.
[b] MAE: Mean Absolute Error.
[c] CMAE: Corrected Mean Absolute Error.

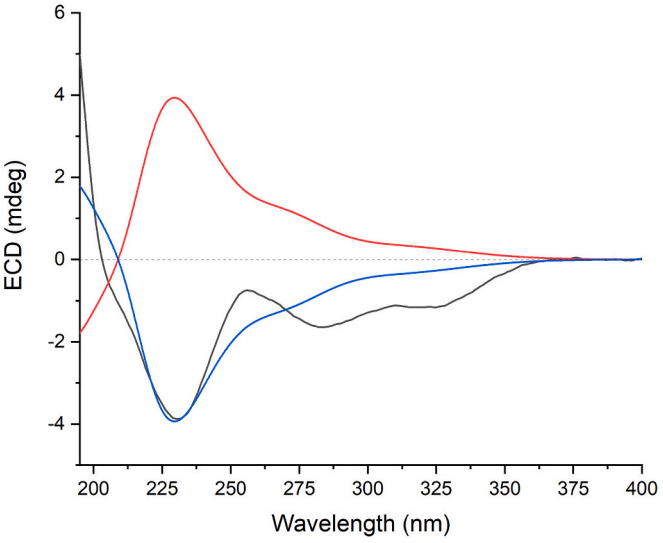

Fig. 5. Experimental ECD spectrum of **5** (black). Calculated ECD spectra of (4*S*,5*S*,6*S*,7*S*)-**5** (**5a**) (shift = 9 nm, red) and (4*R*,5*R*,6*R*,7*R*)-**5** (*ent*-**5a**) (shift = 9 nm, blue). (For interpretation of the references to colour in this figure legend, the reader is referred to the web version of this article.)

The planar structure of **5** was determined by a combined analysis of the 2D NMR spectra. One spin system H-2/H-3/H-4/H-5/H-6/H-7/H-10 could be undoubtedly determined by tracking correlations in the ^{1}H-^{1}H COSY spectrum (Fig. 4). The linkages of all the carbon atoms were further deduced by the critical HMBC experiment (Fig. 4). The HMBC correlations from H-3 (δ_H 6.75) to C-1 (δ_C 199.6), C-4 (δ_C 31.4) and C-5 (δ_C 53.0), from H-2 (δ_H 6.08) to C-4 and C-6 (δ_C 72.6), and from H-6 (δ_H 4.30) to C-1, C-4, C-5, indicated the presence of the α,β-unsaturated cyclohexenone. The HMBC correlations from H-10 (δ_H 1.02) to C-3 (δ_C 157.4), C-4, C-5 and the coupling between H-10 and H-4 (δ_H 3.03) revealed that 10-CH_3 was attached to C-4. Further comparison of its NMR spectral data with those of the known compound, arthropsadiol C [33], indicated that they had the same cyclohexenone moiety and differed only in the side chain. The side chain was determined by the HMBC correlations of H-7 (δ_H 4.66) with C-4, C-5, C-6 and C-8 (δ_C 211.4), and H-9 (δ_H 2.32) with C-7 (δ_C 75.5) and C-8. Thus, the planar structure of compound **5** was determined.

The large coupling constants of 12.4 Hz between H-5 and H-6 implied their *trans*-relationship. The NOE cross-peaks from H-4 to H-6, and from H-5 to H_3–10, supported the *cis*-relationships of H-4 with H-6, and CH_3–10 with H-5. The relative configuration of C-7, as well as the absolute configuration of **5** was determined through quantum chemical

Table 4
Antimicrobial activities of four compounds against different pathogens.

Compounds	MIC (μg/mL)				
	MRSA	*S. aureus*	*S. typhimurium*	*B. cinerea*	*F. graminearum*
4	16	>512	>512	64	64
6	64	64	128	64	32
11	4	4	4	32	16
12	16	32	4	512	32
Nystatin	–	–	–	16	8
Chloramphenicol	4	4	4	–	–

–: No activity.

calculation. To be specific, two candidate structures of **5**, (4*S**,5*S**,6*S**,7*S**)-**5** (**5a***) and (4*S**,5*S**,6*S**,7*R**)-**5** (**5b***) were subjected to quantum chemical calculation of chemical shifts at mPW1PW91-SCRF/6–31 + G(d,p) (IEFPCM, chloroform)//M06–2×-D3/def2-TZVP level of theory. As a result, the calculated chemical shifts of **5a*** were found to match their experimental counterparts better than those of **5b*** (Table 3). Subsequently, (4*S*,5*S*,6*S*,7*S*)-**5** (**5a**) was subjected to TDDFT ECD calculation at PBE0-SCRF/def2-TZVP (IEFPCM, chloroform)//M06–2×-D3/def2-TZVP level of theory, and the calculated curve appeared as nearly a mirror image of the experimental curve (Fig. 5). Thus, the absolute configuration of **5** was determined to be 4*R*, 5*R*, 6*R*, and 7*R*. The structure of compound **5** was shown in Fig. 1, and given the trivial name arthropsadiol D.

Compound **6** was assigned the molecular formula of $C_{10}H_{10}O_2$ by HRESIMS at *m/z* 163.0761 $[M + H]^+$ (calcd for $C_{10}H_{11}O_2$, 163.0759), indicating the existence of six degrees of unsaturation. The ^{1}H NMR spectrum (Table 2) exhibited signals for three aromatic protons at δ_H 6.83, 6.97, and 7.08, an oxymethine proton at δ_H 4.93 (q, $J = 7.0$ Hz) and two methyl groups at δ_H 1.27 (d, $J = 7.0$ Hz) and 2.28 (s). The ^{13}C NMR spectrum showed a carbonyl carbon (δ_C 206.3), three quaternary carbons (δ_C 127.9, 136.7, and 155.0), three olefinic methines (δ_C 114.3, 118.1, and 132.4), an oxymethine (δ_C 70.7), and two methyl groups (δ_C 18.3 and 19.0). The HMBC correlations were observed from H-3 to C-7 and C-8, from H-6 to C-4, C-5 and C-8, and from H-4 to C-5, C-6 and C-8, indicating the presence of 1,2,5-trisubstituted benzene ring. The HMBC correlations from H_3–10 to the quaternary carbon C-5 confirmed the location of the methyl group at C-5 in benzene ring. Since one benzene ring and one carbonyl group accounted for five degrees of unsaturation, the remaining one revealed the presence of a single ring in **6**. The HMBC correlations from H-6 to C-1, from H_3–9 to C-1 and C-2 confirmed the furanose unit. The optical rotation value of **6** was determined to be positive. Thus, compound **6** was identified as (+)-2,5-dimethyl-3(2H)-benzofuranone. This compound was first obtained by synthesis in 1977 [34] and was later reported as an intermediate during the synthesis of 2,3,4-trihydrobenzofurane [35]. In this paper, compound **6** was isolated from natural source for the first time and was a new natural product.

Four compounds were tested for their antimicrobial activities including MRSA, *S. aureus*, *S. typhimurium*, *B. cinerea*, and *F. graminearum* (Table 4). The rest compounds are too limited in the amount to be tested for their bioactivity. The minimal inhibitory concentrations (MICs) were determined by the broth microdilution method. Among them, compound **4** exhibited moderate inhibitory activity against MRSA with MIC value of 16 μg/mL, and displayed only weak antimicrobial activity against *B. cinerea* and *F. graminearum* with MIC values of 64 μg/mL. Compound **6** showed antimicrobial activity against MRSA, *S. aureus*, *B. cinerea* and *F. graminearum* with MIC values of 64, 64, 64 and 32 μg/mL, respectively. Compound **11** displayed most potent antimicrobial activity against MRSA, *S. aureus*, *S. typhimurium*, *B. cinerea* and *F. graminearum* with MIC values of 4, 4, 4, 32 and 16 μg/mL, respectively. Besides, compound **12** exhibited antimicrobial activity against MRSA, *S. aureus*, *S. typhimurium* and *F. graminearum* with MIC values of 16, 32, 4, and 32 μg/mL.

In this study, two new nucleosides (**1** and **2**), one new cyclohexenone derivative (**5**), and a new natural product (**6**), along with eleven known compounds were isolated from the endophytic fungus *Aspergillus polyporicola* R2. The results showed the structural diversity of the secondary metabolites from the strain, mainly involved unique nucleoside derivatives (**1**–**4**), alkaloids (**8** and **9**), and various polyketides including cyclohexanones (**5** and **7**), benzofurane (**6**), and macrolides (**10**–**15**). The nucleoside derivatives (**1**–**4**) consist of uracil, furanose, and aromatic moieties. Kipukasins H (**3**) and I (**4**) were previously isolated from the marine-derived fungus *Aspergillus versicolor* and showed antibacterial activity against *Staphylococcus epidermidis* [24]. Both compounds **5** and **7** are cyclohexanone derivatives, in which the pentalactone of **7** occurred ring-opening. Compounds **7**, **12**, **14**, and **15** were isolated from the genus *Aspergillus* for the first time. In this study, compound **11** showed inhibitory activity against MRSA, *S. aureus* and *S. typhimurium*, and compound **12** also showed inhibitory activity against *S. typhimurium*, with all of the MIC values of 4 μg/mL, which were identical to that of the positive control chloramphenicol. These results suggested that compounds **11** and **12** might be potential antibacterial agents.

Author statement

All authors have read and agreed to the published version of the manuscript.

CRediT authorship contribution statement

Si-Si Liu: Conceptualization, Investigation, Methodology, Writing – original draft, Formal analysis, Data curation. **Rong Huang:** Formal analysis, Data curation. **Shou-Peng Zhang:** Investigation, Methodology. **Kun Hu:** Formal analysis, Data curation. **Shao-Hua Wu:** Supervision, Writing – review & editing.

Declaration of Competing Interest

None.

Data availability

Data will be made available on request.

Acknowledgements

This research was financially supported by the National Natural Science Foundation of China (grant No. 81860634 and No. 32260110); the Applied Basic Research Key Project of Yunnan Province (grant No. 202001BB050029 and No. 202201BF070001-003); the Project of Innovative Research Team of Yunnan Province (grant No. 202005AE160005).

Appendix A. Supplementary data

Supplementary data including 1D and 2D NMR, HRESIMS, and IR

spectra of compounds **1**/**2**, **5** and **6**, and the details for quantum chemical calculations can be found online at https://doi.org/10.1016/j.fitote.2022.105297

References

[1] O. Petrini, Fungal Endophytes of Tree Leaves, Springer, New York, 1991, pp. 179–197.
[2] E. Ancheeva, G. Daletos, P. Proksch, Bioactive secondary metabolites from endophytic fungi, Curr. Med. Chem. 27 (11) (2020) 1836–1854.
[3] D. Nair, S. Padmavathy, Impact of endophytic microorganisms on plants, environment and humans, Sci. World J. (2014) 1–11.
[4] A.F. Tawfike, R. Tate, G. Abbott, L. Young, C. Viegelmann, M. Schumacher, M. Diederich, R. Edrada-Ebel, Metabolomic tools to assess the chemistry and bioactivity of endophytic *Aspergillus* strain, Chem. Biodivers. 14 (10) (2017).
[5] D.A. Tchokponhoué, E.G. Achigan-Dako, S. N'Danikou, D. Nyadanu, R. Kahane, A. O. Odindo, J. Sibiya, Comparative analysis of management practices and end-users' desired breeding traits in the miracle plant [*Synsepalum dulcificum* (Schumach & Thonn.) Daniell] across ecological zones and sociolinguistic groups in West Africa, J. Ethnobiol. Ethnomed. 17 (2021) 1–20.
[6] G.E. Inglett, D.J. Chen, Contents of phenolics and flavonoids and antioxidant activities in skin, pulp and seeds of miracle fruit, J. Food Sci. 76 (3) (2011) 479–482.
[7] Y.C. Han, J.Y. Wu, C.K. Wang, Modulatory effects of miracle fruit ethanolic extracts on glucose uptake through the insulin signaling pathway in C2C12 mouse myotubes cells, Food Sci. Nutr. 7 (3) (2019) 1035–1042.
[8] W. Huang, H.Y. Chung, W. Xuan, G. Wang, Y. Li, The cholesterol-lowering activity of miracle fruit (*Synsepalum dulcificum*), J. Food Biochem. 44 (5) (2020).
[9] S. Afzal, A.V. Raju, C.S. Raju, G. Chong, Evaluation of the antimicrobial and anticancer properties of the fruits of *Synsepalum dulcificum* (Sapotaceae), Trop. J. Pharm. Res. 20 (9) (2021) 1925–1930.
[10] H. Wasoh, S. Tajuddin, M. Halim, A.R. Mohd-Hairul, M.Z.M. Sobri, A.F.B. Lajis, M. T. Yusof, A.B. Ariff, Antibacterial activity of *Synsepalum dulcificum* leaf extract against *Listeria monocytogenes* and its comparison with *Strobilanthes crispus* and *Morus alba*, J. Biosci. 25 (2017) 73–75.
[11] J. Seong, G. Oyong, E. Cabrera, *Synsepalum dulcificum* extracts exhibit cytotoxic activity on human colorectal cancer cells and upregulate c-fos and c-jun early apoptotic gene expression, Asian Pac. J. Trop. Biomed. 8 (3) (2018) 173–178.
[12] S. Guney, W.W. Nawar, Seed lipids of the miracle fruit (*Synsepalum Dulcificum*), J. Food Biochem. 1 (2) (1977) 173–184.
[13] L.Q. Du, Y.X. Shen, X.M. Zhang, Antioxidant-rich phytochemicals in miracle berry (*Synsepalum dulcificum*) and antioxidant activity of its extracts, Food Chem. 153 (2014) 279–284.
[14] C.Y. Chen, Y.D. Wang, H.M. Wang, Chemical constituents from the leaves of *Synsepalum dulcificum*, Chem. Nat. Compd. 46 (3) (2010) 495.
[15] M.J. Cheng, Z.L. Hong, C.Y. Chen, Secondary matabolites from the stem of *Synsepalum dulcificum*, Chem. Nat. Compd. 48 (1) (2012) 108–109.
[16] F. He, J. Bao, X.Y. Zhang, Z.C. Tu, Y.M. Shi, S.H. Qi, Asperterrestide A, a cytotoxic cyclic tetrapeptide from the marine-derived fungus *Aspergillus terreus* SCSGAF0162, J. Nat. Prod. 76 (6) (2013) 1182–1186.
[17] R. Haritakun, P. Rachtawee, R. Chanthaket, N. Boonyuen, M. Isaka, Butyrolactones from the fungus *Aspergillus terreus* BCC 4651, Chem. Pharm. Bull. 58 (11) (2010) 1545–1548.
[18] H.B. Huang, Z.E. Xiao, X.J. Feng, C.H. Huang, X. Zhu, J.H. Ju, M.F. Li, Y.C. Lin, L. Liu, Z.G. She, Cytotoxic naphtho-γ-pyrones from the mangrove endophytic fungus *Aspergillus tubingensis* (GX1-5E), Helv. Chim. Acta. 94 (2011) 1732–1740.
[19] T. He, Y.D. Wang, L.Q. Du, F.R. Li, Q.F. Hu, G.G. Cheng, W.G. Wang, Overexpression of global regulator *LaeA* induced secondary metabolite production in *Aspergillus versicolor* 0312, Rec. Nat. Prod. 14 (6) (2020) 387–394.
[20] K.T. Bergh, A.A. Brakhage, Regulation of the *Aspergillus nidulans* penicillin biosynthesis gene *acvA* (*pcbAB*) by amino acids: implication for involvement of transcription factor PACC, Appl. Environ. Microbiol. 64 (3) (1998) 843–849.
[21] J. Choochuay, X. Xu, V. Rukachaisirikul, P. Guedduaythong, S. Phongpaichit, J. Sakayaroj, J. Chen, X. Shen, Curvularin derivatives from the soil-derived fungus *Aspergillus polyporicola* PSU-RSPG187, Phytochem. Lett. 22 (2017) 122–127.
[22] C. Wang, K.H.A.U. Zaman, A.M. Sarotti, X.H. Wu, S.L. Zheng, S.G. Cao, NF-κB inhibitory, antimicrobial and antiproliferative potentials of compounds from Hawaiian fungus *Aspergillus polyporicola* FS910, 3, Biotech. 11 (8) (2021), 391–340.
[23] P. Jiao, S.V. Mudur, J.B. Gloer, D.T. Wichlow, Kipukasins, nucleoside derivatives from *Aspergillus Versicolor*, J. Nat. Prod. 70 (8) (2007) 1308–1311.
[24] M. Chen, X.M. Fu, C.J. Kong, C.Y. Wang, Nucleoside derivatives from the marine-derived fungus *Aspergillus versicolor*, Nat. Prod. Res. 28 (12) (2014) 895–900.
[25] M.Y. Su, S.X. Chen, X.Z. Liu, Y.H. Pei, I.-K. Trichocladinols, Oxatricyclic and oxabicyclic polyketides from *Trichocladium opacum*, Nat. Prod. Commun. 9 (5) (2014) 695–698.
[26] Y. Wang, J.K. Zheng, P.P. Liu, W. Wang, W.M. Zhu, Three new compounds from *aspergillus terreus* PT06-2 grown in a high salt medium, Mar. Drugs. 9 (8) (2012) 1368–1378.
[27] W.G. Sun, X.T. Chen, Q.Y. Tong, Novel small molecule 11β-HSD1 inhibitor from the endophytic fungus *Penicillium commune*, Sci. Rep. 6 (2016) 26418.
[28] M. Kusano, K. Nakagami, T. Kawano, Y. Kimura, *βγ*-Dehydrocurvularin and related compounds as nematicides of *Pratylenchus penetrans* from the fungus *Aspergillus* sp, Biosci. Biotechnol. Biochem. 67 (6) (2003) 1413–1416.
[29] S.B. Hyeon, A. Ozaki, A. Suzuki, T. Saburo, Isolation of *αβ*-dehydrocurvularin and *β*-hydroxycurvularin from *Alternaria tomato* as sporulation-suppressing factors, Agric. Boil. Chem. 40 (8) (1976) 1663–1664.
[30] A.H. Aly, A. Debbab, C. Clements, R.A. Edrada-Ebel, B. Orlikova, M. Diederich, Nf kappa B inhibitors and antitrypanosomal metabolites from endophytic fungus *penicillium* sp. isolated from *Limonium tubiflorum*, Bioorg. Med. Chem. 19 (1) (2011) 414–421.
[31] C.G. Pierce, P. Uppuluri, A.R. Teistan, J.F.L. Wormley, E. Mowat, G. Ramage, J. L. Lopez-Ribot, A simple and reproducible 96-well plate-based method for the formation of fungal biofilms and its application to antifungal susceptibility testing, Nat. Protoc. 3 (9) (2008) 1494–1500.
[32] M.D. Jackson, J.M. Denu, Structural identification of 2′- and 3′-*O*-acetyl-ADP-ribose as novel metabolites derived from the sir2 family of *β*-NAD^+-dependent histone/protein deacetylases, J. Biol. Chem. 277 (21) (2002) 18535–18544.
[33] G.F. Zhang, W.B. Han, J.T. Cui, S.W. Ng, Z.K. Guo, R.X. Tan, H.M. Ge, Neuraminidase inhibitory polyketides from the marine-derived fungus *Phoma herbarum*, Planta Med. 78 (1) (2012) 76–78.
[34] L. Caranti, G. Zecchi, U.M. Pagnoni, Anionotropic shift of the 3-substituent in the reaction of 2-methoxy-2,3-dihydro-3-benzofuranols with boron trifluoride, J. Heterocyclic Chem. 14 (3) (1977) 445–448.
[35] M. Deshmukh, D. Kharade, S.D. Shirke, A short synthesis of 2,3,4-trihydrodibenzofuranes, Monatsh. Chem. 125 (8) (1994) 971–976.